42. M. Jacquin and J. Millet, *C. R. Acad. Sci., Paris*, **266**, 25 (1968).
43. J.-P. Loup, Z. Mihailovic, and P. Morvan, *C. R. Acad. Sci., Paris*, **261**, 109 (1965).
44. A. Wilcockson and R. E. W. Casselton, *J. Am. Ceram. Soc.*, **53**, 293 (1970).
45. C. Beranger and P. Lacombe, *Rev. Int. Hautes Temp. Refract.*, **3**, 235 (1966).

Technical Notes

Thin Film Analysis of Photomask Coatings

G. E. McGuire,* T. D. Metzgar,* R. V. Shah, and R. C. Bracken*

Texas Instruments Incorporated, Dallas, Texas 75222

Photolithographic processing of semiconductor products requires the use of high quality masking materials to define certain features of the device. Other than the requirement that the masking material must be capable of blocking the actinic radiation (predominantly u.v.) necessary for photoresist work, the requirements for masking materials can be quite varied. The basic requirements are that the film be durable, scratch resistant, thermally stable, adhere well to glass and yet be resistant to attack by organic cleaners or solvents, and free from pinholes (1).

The most commonly used material is 700-1000Å chromium on soda-lime or borosilicate glass plates. The Cr film mask was originally a substitute for the photographic emulsion mask because the opaque layer was thinner, harder, and better defined.

The trend toward smaller geometries in very large scale integration (VLSI), coupled with electron-beam fabrication of master masks (2) and projection printing, have increased the demands on the masking material. The trend toward VLSI puts a high premium on low defect density and pinhole free material. Increasing complexity and use of positive resist has resulted in a greater number of masks which are mostly opaque and therefore more difficult to align. This has accelerated the trend toward see-through materials which allow direct observation of the most critical elements of a device pattern. In addition, halation effects are minimized due to absorption of the unwanted light rather than reflection. Iron oxide (3-5), V_2O_5, (6) and NiO (6) are some of the materials which have been investigated for see-through masks. Antireflective chromium (7), chromium oxide, may also be used to reduce reflectivity, but it is not transparent to visible radiation. Other antireflective coatings of CeO_2, TiO_2, CeF_3, $PbTiO_3$, ZnO, and $GaFeO_3$ have been investigated for use in conjunction with chromium masks (8).

For any of these materials one must maintain careful control of the chemical and physical composition. Small changes in the composition of the film may result in large variations in the optical density of the deposit (9), or variations in etch rate (1). If the etch rate is nonuniform over the surface of the mask or varies from lot to lot, then patterning of the plates may result in removal of certain features due to overetching. The thickness of the films (700-1000Å) permits compositional analysis by only a few analytical techniques for which the signal originates in the top few hundred angstroms of material. Auger and photoelectron spectroscopy combined with in-depth profiling have been used to investigate composition variations in Cr, Si_3N_4, SiC, and Si photomask coatings. In both AES and XPS the sampling depth is only 15-60Å (10).

Experimental

Both AES and XPS analysis were performed in a combined AES/XPS spectrometer, with a double pass cylindrical mirror analyzer produced by Physical Electronics Incorporated. Auger excitation was accomplished using a 5 keV, 5 μA electron beam with a spatial resolution of 25μ. The spectra were recorded using a 3 or 6 eV pp modulation voltage, 0.3 sec time constant, and 3 eV/sec sweep rate. Photoelectron spectra were excited with $AlK\alpha_{1,2}$ radiation with the x-ray anode operated at 10 kV and 60 mA. Survey scans were taken at 200 eV pass energy and high resolution data were taken at 25 or 50 eV pass energy.

After sampling the surface composition, in-depth profiling was accomplished by sputtering with 2 keV Kr^+ at 3.8×10^{-3} Pascal.

Chromium films were sputter-deposited from a Materials Research Corporation Model 8800 sputtering system onto 60-90 mil soda-lime glass plates. The Cr source was an 18 in. Marz-grade chromium target sputtered in an argon ambient of 8μ. The base pressure prior to deposition was less than 1×10^{-5} Torr. The main chamber was turbomolecular, pumped with a liquid nitrogen cold-trap. The load lock was mechanically pumped to 70μ before the glass plates were transferred into the main chamber. The target was water cooled and the plates were not intentionally heated during deposition.

Results and Discussion

The compatibility of chromium with photolithographic processing has kept it one of the leading mask materials. It has versatile etchability and good edge definition. Yet careful control must be maintained over the deposition process in order to insure a uniform etch rate either by conventional wet etching or plasma etching. Until recently, resistivity measurements were used as the main means of determining the effect of deposition and postdeposition conditions on thin film variations. Janus (11) has investigated the deposition parameters of rf sputtered chromium using chemical etch rate studies. Although chemical etch rate tests provide valuable information on deposition parameters, they do not determine the actual film composition.

Both physical and chemical changes may occur in the deposited chromium films which may affect the etch rate and subsequently complicate patterning for photomask production. Chemical composition of the films may be determined by either AES or XPS. Both

* Electrochemical Society Active Member.
Key words: films, etching, photolithography.

AES and XPS are sensitive to carbon (low molecular weight hydrocarbons) oxygen and nitrogen, the most common impurities which may be incorporated in the deposited Cr. An examination of the surface reveals little information because of the tendency to form a thin native oxide on exposure to air. It is not until the surface oxide has been removed by ion sputtering that variations in film composition can be observed. Figure 1 shows the Auger spectra of Cr films deposited with and without the use of a cold-trap in a turbomolecular pumped MRC system. The use of a cold-trap and orifice in a system pumped to a base pressure of 5×10^{-6} Torr is sufficient to prevent the incorporation of other than trace C and N in the Cr. The O(510 eV) transition occurs between the Cr(529 eV) and Cr(571 eV) transitions but appears to be virtually absent. Even without the use of a liquid N_2 cold-trap and orifice, the level of C and O incorporated in the Cr increases only slightly when a low base pressure is maintained in the sputtering system. Near the Cr/glass interface there is a sharp increase in the amount of O in the film.

An in-depth profile of a Cr film to the Cr/glass interface shows the composition of a film that was deposited under good conditions. Figure 2 shows the distribution of C, N, O, Cr, and Si in the 700Å Cr films

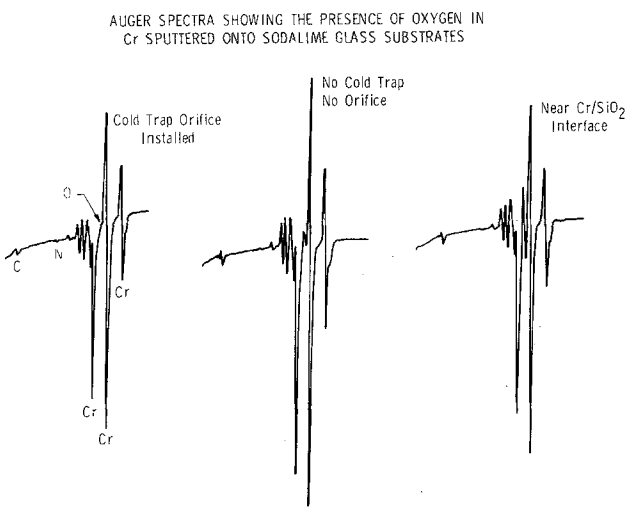

Fig. 1. The Auger spectra of chromium photomask show the low levels of C, N, and O incorporated in the Cr during deposition with and without the use of a liquid nitrogen cold-trap and orifice. The O signal increases near the Cr/glass interface due to reaction of Cr with the substrate during deposition.

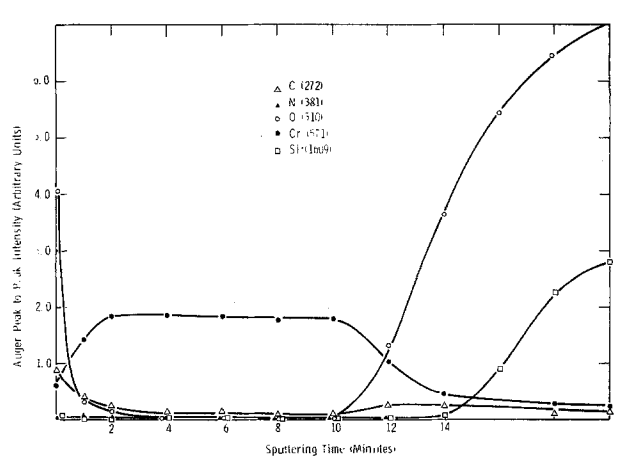

Fig. 2. An in-depth profile of a Cr film to the Cr/glass interface shows the distribution of C, N, O, Cr, and Si. The initial surface is covered with a native oxide and some C residue. The interior of the Cr is virtually free of any C, N, and O. Near the interface the O signal begins to increase before the Si increases, suggesting that a layer of Cr oxide is formed during deposition.

by plotting the Auger peak-to-peak intensity as a function of sputtering time. The initial surface is covered with a native oxide and some C residue. The surface C and O are quickly removed, revealing a Cr layer which is virtually free of any C, N, or O. Near the interface the O signal begins to increase and does not level off until within the glass substrate.

The increase in O before the appearance of Si suggests the formation of an oxide layer of Cr at the interface. Frieser (12) found the original glass surface may have become modified during the chromium deposition process, in which case an interfacial region rather than a sharp interface is expected. Frieser made his observations by measuring the contact angle that drops of water form with the respective surfaces. In the Auger profiles the change in going from surface oxide, to metallic Cr, to Cr oxide, to mixed Cr oxide-glass, then to glass may be observed by following the intensities of the various Auger transitions while ion milling the surface. In addition, the oxidation state of the Cr may be determined by ESCA analysis. Within the 700Å Cr film a photoelectron binding energy of 574.7 eV is observed for the Cr 2p3/2 transition which is in agreement with that of Cr metal (13). At the Cr/glass interface, the Cr 2p3/2 binding energy shifts from 2.3 to 577.0 eV which corresponds to Cr_2O_3. The adhesion of Cr to glass is enhanced by the chemical reaction of the metal to the substrate, and results in a bond that is stronger than the cohesive forces in the glass (12). Most theories of metal film adhesion consider a metal-oxide-substrate interface layer to be a dominant factor with a number of other parameters affecting thin film adhesion to a smaller extent. These include the substrate cleaning procedure, the rate of deposition, the film thickness, the type of substrate, the substrate temperature, the purity of source material, and the pressure in the evaporator during deposition (14). The attack on chromium oxide at the Cr/glass interface by soda-lime glass substrates can also lead to long term instability (7).

Occasionally, impurities become incorporated in the Cr deposit affecting both the Cr adhesion to the glass substrate and the etching characteristics of the film. The two most common sources of impurities are residual contamination on the glass substrate or sputtering target surface, and background gases in the sputtering ambient. These are usually low molecular weight hydrocarbons from solvents, pump oil, oxide films or O_2 and H_2O background gases. In Fig. 3 are the Auger spectra of two different Cr films on glass substrates that were sputtered until any native oxide was removed. It can be seen that quite high concentrations of C, N, and O may become incorporated in the Cr deposit. The contaminants are not merely trapped in the film but react chemically just as the Cr reacted with the glass substrate. This is demonstrated by the shape of the C Auger transition which is characteristic of carbide formation (15).

The load lock of the sputtering system is backfilled with N_2 then evacuated to 70μ when fresh substrates are loaded into the sputtering chamber. It is suspected that some N_2 passes into the main chamber and is mixed with Ar during the sputtering of Cr. Rather than sputtering at 8μ of pure Ar, sputtering occurs in a N_2/Ar mixture, resulting in the incorporation of N into the Cr film as in Fig. 3B. An air leak is not suspected because the O signal is still very small. Since the chemical reactivity of O is much greater than N, an air leak would result in the incorporation of more O than N in the Cr.

Profiling of the film, Fig. 4, reveals the presence of N throughout the Cr deposit. The C concentration is high at the surface but is reduced within the Cr, then increases again at the interface. The increase of C at the interface may be due to improper cleaning of the glass plates prior to loading into the sputtering system

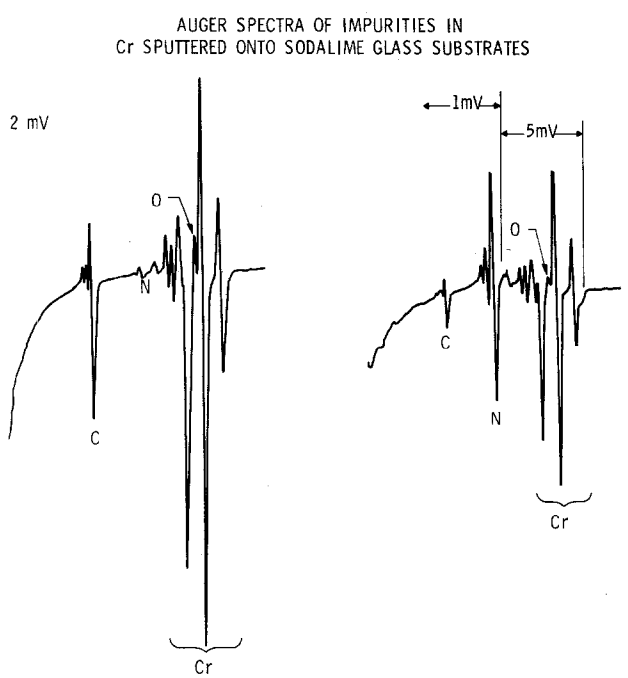

Fig. 3. The Auger spectra of two different Cr films show the incorporation of C and N in the film during deposition. The characteristic shape of the C signal is that of a carbide which indicates the contaminants are not merely trapped in the film but react chemically with the Cr.

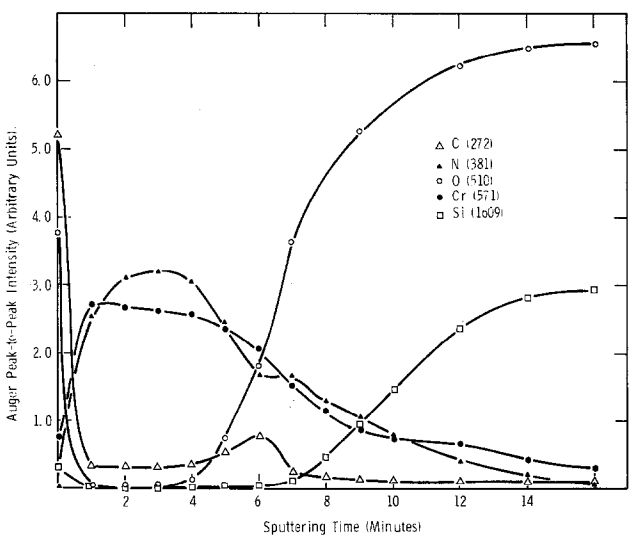

Fig. 4. An in-depth profile of the photomask from Fig. 3B shows the distribution of N, C, and O throughout the Cr film. The distribution of N throughout the film is a result of N_2 in the sample load lock mixing with the Ar sputtering gas when the sample is moved into the deposition chamber. The presence of a high C signal at the Cr glass interface is attributed to contamination of the Cr target or solvent residues on the glass plate.

or solvent residues on the glass surface. In this particular example, the source of C is suspected to be within the sputtering chamber since C is found throughout the Cr deposit.

Instead of Cr_2O_3 then Cr_2O_3/SiO_2 at the interfacial region, there is a layer rich in C, N, O, and Cr. Whereas rupture of a clean Cr deposit on glass is expected to occur within the glass, the weak point in systems like this is frequently the region of highest C concentration. Plasma etching or wet chemical etching of the film is difficult to control due to the varying chemical composition of the film as a function of depth.

The excitation of AES transitions with an electron beam can become difficult with insulating samples.

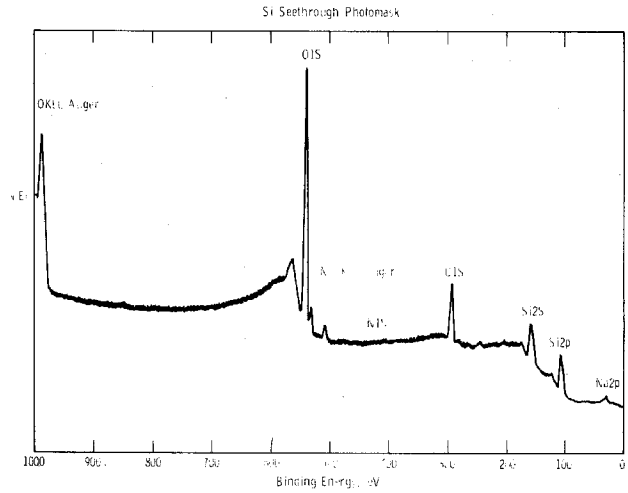

Fig. 5. Silicon is used as a see-through photomask material since it is transparent in the visible yet blocks the actinic radiation. Silicon on glass is a good insulator so excitation of Auger spectra with an electron beam becomes difficult. Shown here is an x-ray excited photoelectron spectrum of a Si photomask showing both the Auger and photoelectron transistors of O, Na, C, N, and Si.

If an insulating layer is used in the manufacture of photomask over the 60-90 mil glass, then XPS becomes the technique most useful for analysis. Figure 5 shows the photoelectron spectrum of a Si see-through photomask. The XPS spectrum of the outer Si surface reveals the presence of a native oxide, residual hydrocarbon contamination, and Na, which may originate from handling. The transparency of Si in the visible region of the spectrum allows see-through alignment of the mask while blocking the actinic radiation.

Even though Cr fulfills the major requirements of a photomask coating, there are ways to protect the Cr surface from damage during contact printing and extend its useful life. One method is to apply a soft or lubricating material to the surface (16) or alternatively through the use of an ultrahard protective overcoat such as Si_3N_4 or SiC. R. S. Horwath *et al.* (17) have demonstrated that reactively sputtered Si_3N_4 reduces star cracking caused by epi spikes by 30% without adversely affecting images produced in photoresist. The basic requirements of such a film is that it protects the mask from damage, that it be transparent between 330 and 550 nm, and that it is nearly defect-free.

In this study sputtered silicon nitride and silicon carbide films were investigated for overcoating photomasks. Auger spectroscopy combined with ion sputtering was found as one of the best means of monitoring the composition of the films. Carbon and oxygen were usually found as impurities in the nitride films, and oxygen was found as an impurity in carbide films unless extreme care was taken to clean the deposition chamber. This is a problem which is frequently encountered with plasma-deposited (18) and chemically vapor-deposited films (19).

The Auger peak-to-peak intensity ratio of Si to C in the carbide films and Si to N in the nitride films was found to vary depending on the Ar sputtering pressure. In actual practice the sputtered silicon carbide was not satisfactory as a coating material. At 6μ sputtering pressure in Ar, the deposited silicon carbide resisted abrasion but absorbed too much in the u.v. region. At higher sputtering pressures the coating was easily abraded but had acceptable optical transmission. At the same sputtering pressure, silicon nitride has approximately the same abrasion resistance as silicon carbide but the nitride is less opaque in the u.v. Also, the optical characteristics of the nitride films can be adjusted by sputtering in an Ar-N_2 mixture. The refractive index of films sputtered in an

Table I. Silicon nitride sputtered from silicon nitride target in N_2/Ar mixture

%N_2	Pressure (m Torr)	Index of refraction	Auger peak-to-peak intensity ratio Si/N
0	6	2.35	0.51
20	6	1.85	0.35
25	6	1.88	0.39
33	6	1.81	0.32
25	6	1.88	0.39
25	10	1.77	0.34
25	25	1.68	0.47

Ar-N_2 mixture follows the trend observed in the Si to N Auger intensity ratio. The results for a series of runs at different Ar-N_2 compositions are listed in Table I. A mixture of 25% N_2 in Ar at 6μ was found to give the optimum optical transmission and abrasion resistance.

Conclusion

Auger and photoelectron spectroscopy have been utilized in the evaluation of a variety of thin film coatings used in the manufacture of photomasks. The shallow sampling depth and sensitivity of these techniques for low atomic number elements were instrumental in identifying the presence of C, N, and O residues in Cr photomasks which affect the etching characteristics of the photomask during patterning.

In-depth profiling reveals the interfacial composition of Cr on glass consists of mixed oxides of Cr and Si. The deposition of Cr results in oxidation of a thin layer of Cr which promotes adhesion of the Cr to the glass.

Hard protective overcoats of silicon carbide and silicon nitride were evaluated by AES and ellipsometry to arrive at the proper sputtering pressure and gas composition to give the optimum optical transmission and abrasion resistance.

Manuscript submitted Nov. 6, 1978; revised manuscript received Dec. 11, 1978.

Any discussion of this paper will appear in a Discussion Section to be published in the December 1979 JOURNAL. All discussions for the December 1979 Discussion Section should be submitted by Aug. 1, 1979.

Publications costs of this article were assisted by Texas Instruments, Incorporated.

REFERENCES

1. R. E. Szupillo, *Solid State Technol.*, 49 (July 1969).
2. J. P. Ballantyne, *J. Vac. Sci. Technol.*, **12**, 1257 (1975).
3. M. V. Sullivan, *This Journal*, **120**, 545 (1973).
4. W. R. Sinclair, D. L. Rousseau, and J. J. Stancavish, *ibid.*, **121**, 925 (1974).
5. D. R. Mason, *ibid.*, **123**, 519 (1976).
6. W. R. Sinclair, M. V. Sullivan, and R. A. Fastnacht, *ibid.*, **118**, 341 (1971).
7. W. H. Kroeck and T. H. Briggs, Proceedings of the 1970 Kodak Seminar on Microminiaturization, San Diego, California, 1970.
8. V. Sadagopan, *IBM Technical Disclosure Bulletin*, **14**, No. 3, 795 (1971).
9. G. Henderson and C. Weaver, *J. Opt. Soc. Am.*, **56**, 1551 (1966).
10. T. A. Carlson and G. E. McGuire, *J. Electron Spectrosc. Relat. Phenom.*, **1**, 161 (1972).
11. A. R. Janus, *This Journal*, **119**, 392 (1972).
12. R. G. Frieser, *ibid.*, **119**, 360 (1972).
13. T. A. Carlson, "Photoelectron and Auger Spectroscopy," p. 358, Plenum Press, New York (1975).
14. N. M. Poley and H. L. Whitaker, *J. Vac. Sci. Technol.*, **11**, 114 (1974).
15. J. T. Grant and T. W. Haas, *Phys. Lett.*, **33A**, 386 (1970).
16. D. L. Flowers, *This Journal*, **124**, 1608 (1977).
17. R. S. Horwath, J. G. Horvat, and V. Sadagopan, Abstract 4, p. 16, The Electrochemical Society Extended Abstracts, Vol. 74-1, San Francisco, Calif., May 12-17, 1974.
18. S. Thomas and R. J. Mattox, *This Journal*, **124**, 1942 (1977).
19. P. H. Holloway and H. J. Stein, *ibid.*, **123**, 723 (1976).

A Method for Reducing the Hole and Electron Trapping Densities in Thermal SiO_2 Films

S. Iwamatsu and Y. Tarui

VLSI Technology Research Association, Cooperative Laboratories, 4-1-1, Miyazaki, Takatsuku, Kawasaki, 213 Japan

The trapping of charges in insulating films on semiconductors can be a potentially major problem, limiting the miniaturization of VLSI circuits (1, 2). We have been studying a method for the reduction of trapping densities. In this paper, we present new experimental results to estimate and reduce the charge trapping densities in thermal SiO_2 films.

Trapping and Detection Method

A corona charging method to produce hole and electron traps in SiO_2 film on Si has been developed (3). The corona charging method is based on the deposition of negative or positive ions from the corona charging grid on the insulating film of a sample at atmospheric pressure. This results in the application of a high field in the insulating film with no electrode, and introduces the field-induced charge traps in the insulating film on the semiconductor. Trapped holes are produced by negative corona charging, and trapped electrons are produced by positive corona charging of an insulating film. The densities of electron and hole traps are estimated by measuring the *C-V* curve shift after corona charging, using an In-Ga liquid probe.

Key words: VLSI, corona charging, *C-V* curve, phosphorous doping, annealing.

Figure 1 shows *C-V* curves before and after corona charging of (a) 2 min at +8 kV corona charging, (b) 2 min at −8 kV corona charging, and (c) 2 min at +8 kV corona charging after 2 min at −8 kV corona charging of a thermal SiO_2 film which has approximately 50 nm grown in dry oxygen ambient at 1000°C. As can be seen, a high concentration of hole traps is always present in thermally grown SiO_2 and the concentration of electron traps can be made remarkably small. But once holes are trapped by negative corona charging, a high concentration of electron traps are observed.

The distribution of the traps is estimated by *C-V* measurement of the sample for several different oxide thickness obtained by successive etching steps. Analysis of the data gives the position of the centroid of trapped charges. The centroid of the trapped holes lies within